*Chinese Journal of Polymer Science Vol. 35, No. 3, (2017), 372–385*

***Chinese Journal of Polymer Science***


# Synthesis and Properties of Novel Polyimide Fibers Containing Phosphorus Groups in the Side Chain (DATPPO)*

Yong Zhao[a, b], Guo-min Li[a], Fang-fang Liu[a], Xue-min Dai[a], Zhi-xin Dong[a**] and Xue-peng Qiu[a**]

[a] *Polymer Composites Engineering Laboratory, Changchun Institute of Applied Chemistry, Chinese Academy of Sciences, Changchun 130022, China*

[b] *University of Chinese Academy of Sciences, Beijing 100049, China*

**Abstract** A series of polyamic acid copolymers (co-PAAs) containing phosphorous groups in the side chains were synthesized from [2,5-bis(4-aminophenoxy) phenyl] diphenylphosphine oxide (DATPPO) and 4,4′-oxydianiline (ODA) with 3,3′,4,4′-biphenyltetracarboxylic dianhydride (*s*-BPDA) through the polycondensation in *N*,*N*′-dimethyacetamide (DMAc). The co-PAA solutions were spun into fibers by a dry-jet wet spinning process followed by thermal imidization to obtain co-polyimide (co-PI) fibers. FTIR spectra and elemental analysis confirmed the chemical structure of PI fibers. SEM results indicated that the resulting PI fibers had a smooth and dense surface, a uniform and circle-shape diameter. The thermogravimetric measurements showed that with the increase of DATPPO content, the resulting PI fibers possessed high decomposition temperature and residual char yield, indicating that the PI fibers had good thermal stability. The corresponding limiting oxygen index (LOI) values from the experiment results showed that the co-PI fibers possessed good flame-retardant property. Furthermore, the mechanical properties of the co-PI fibers were investigated systematically. When the DATPPO content increased, the tensile strength and initial modulus of the co-PI fibers decreased. However, the mechanical properties were improved by increasing the draw ratio of the fibers. When the draw ratio was up to 2.5, the tensile strength and initial modulus of the co-PI fibers reached up to 0.64 and 10.02 GPa, respectively. The WAXD results showed that the order degree of amorphous matter increased with increased stretching. In addition, the SAXS results displayed that valuably drawing the fibers could eliminate the voids inside and lead to better mechanical property. WAXD revealed that the orientation of the amorphous polymer influenced the mechanical properties of the fibers.

**Keywords** [2,5-Bis(4-aminophenoxy) phenyl] diphenylphosphine oxide; Dry-jet wet spinning process; Phosphorous; Polyimide fibers

**Electronic Supplementary Material** Supplementary material is available in the online version of this article at http://dx.doi.org/10.1007/s10118-017-1896-7.

## INTRODUCTION

Since the first report on polyimide (PI) fibers by Irwin[1] in 1968, this field was developed widely with the contributions from many researchers mainly in the United States, Japan, Russia, and China. As a class of high-performance fibers, the aromatic PI fibers are the most promising engineering materials because of their excellent properties, such as high thermal stability, dimensional stability, excellent mechanical properties, and irradiation resistance. Two major methods, namely, one-step and two-step methods, are generally used to

* This work was financially supported by the National Basic Research Program of China (973 Program, Key Project: 2014CB643604) and the National Natural Science Foundation of China (No. 51373164).

** Corresponding authors: Zhi-xin Dong (董志鑫), E-mail: zxdong@ciac.ac.cn
Xue-peng Qiu (邱雪鹏), E-mail: xp_q@ciac.ac.cn

Received July 15, 2016; Revised August 23, 2016; Accepted September 11, 2016
doi: 10.1007/s10118-017-1896-7

fabricate PI fibers. In the one-step method, PI fibers are directly generated from a soluble PI solution (usually in toxic phenol solvents)[2–7]. Zhang *et al*.[6] reported that the soluble co-polyimide (co-PI) fibers exhibited a strength and modulus of 2.25 and 102 GPa, respectively. Cheng *et al*.[8] prepared a new PI fiber of BPDA/DMB with a strength and modulus of 3.3 and 130 GPa. Although this method is considered as the most effective means to prepare the high-performance PI fibers, the presence of soluble monomers and toxic solvents restricts the industrial production. The two-step method is adopted to overcome the drawbacks mentioned above[9, 10]. By this method, the polyamic acid (PAA) solutions are prepared and extruded followed by thermal[11, 12] or chemical imidization[13] to produce the final PI fibers. Industrial production of PI fibers is likely to use this method because of the extended selection of monomers and solvents. However, microvoids and defects are readily generated during the dual-diffusion process and the thermal imidization. These microvoids and defects cause the decrease of the mechanical properties of PI fibers. A heat-drawing process is generally applied to eliminate the defects of PI fibers resulting from the two-step method.

Recently, PI fibers are widely applied in high-temperature-resistance bag filters (P84®) and fireproof materials, especially in the aerospace field. Traditional PI fibers cannot meet the special demands of flame retardancy and higher-temperature resistance in space or electronic industry. As well known, the element phosphorous is widely utilized as the flame retardants. Currently, phosphorous-containing fibers are synthesized into a matrix in the form of additive fillers to achieve excellent flame retardancy. However, too much filler in the matrix reduced the inherent performance and compatibility with the matrix. Evidently, introducing phosphorous directly into the polymeric structure through copolymerization is a good option. Ding *et al*.[14] incorporated diamine-containing phosphorous into a polymer *via* copolymerization and found that the low phosphorous content in the polymer showed poor flame retardancy. In our previous work[15], we investigated the relationship between the high phosphorous content and the mechanical properties of co-PI fibers by introducing phosphorous to the polymer main chains. The results showed that adding too much phosphorous to the polymer affected the performance of the main chains because of the low bond energy of P—C at high temperatures. As continuation of our previous work, we synthesized a series of co-PI fibers containing phosphorous in the side chains of the polymers, which aimed to maintain the regularity of the main chains and improve the flame retardancy. In a typical manner, a phosphorous-containing diamine monomer (DATPPO) was synthesized and introduced into the side chains of PI through copolymerization. Then, a series of novel co-PI fibers were prepared with the two-step method followed by complete investigation of the properties of the obtained fibers.

## EXPERIMENTAL

### *Chemicals and Materials*

[2,5-Dihydroxyphenyl(diphenyl)phosphine oxide] and 4-chloronitrobenzene were purchased from Jinan Haohua Industry Co., Ltd. and TCI (Shanghai) Development Co., Ltd., respectively. *N*,*N*′-dimethylacetamide (DMAc) was obtained from Tianjin Fu Chen Chemicals Reagent Factory without further purification prior to use. 4,4′-Oxydianiline (4,4′-ODA) and 3,3′,4,4′-biphenyltetracarboxylic dianhydride (*s*-BPDA) were purchased from Shanghai Research Institute of Synthetic Resins. *s*-BPDA was dried overnight in a vacuum at 260 °C prior to use. All the other chemicals were obtained from commercial sources and used as received.

### *Synthesis of [2,5-Bis(4-aminophenoxy) phenyl] diphenylphosphine Oxide*

The monomer of [2,5-bis(4-aminophenoxy) phenyl] diphenylphosphine oxide was synthesized following a procedure described in the literature[16–18]. The typical procedure is shown in Scheme 1 and the details are shown in the supporting information (SI).

### *Synthesis of PAA Spinning Solutions*

For the polymerization, the molar ratios of DATPPO/ODA were varied from 0/10 to 6/4 at 10% increment. For example, when the molar ratio of the diamines was 3/7, 63.53 g (0.129 mol) of DATPPO and 60.27 g (0.301 mol) of ODA were dissolved in DMAc in a nitrogen atmosphere and stirred at room temperature to form a solution. A stoichiometric quantity of dianhydride *s*-BPDA was subsequently added. The solid content was

adjusted to 15% (solid weight to total weight, *W*/*W*). The mixture was stirred at room temperature for 24 h to obtain a viscous PAA solution. The synthetic route is illustrated in Scheme 2. The polymerization procedure at the other ratios of DATPPO/ODA was similar to the aforementioned. The inherent viscosities of the solutions are shown in Table 1. The viscosity values decreased with increase of the DATPPO content.

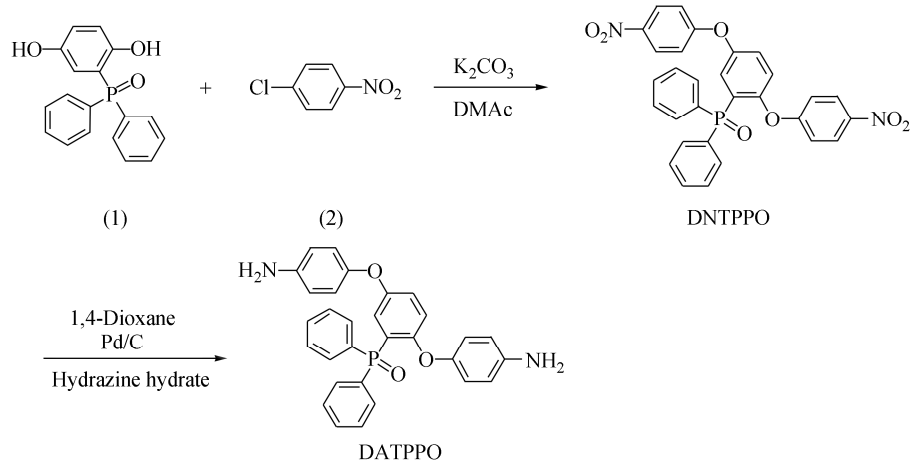


**Scheme 1** Synthetic route to [2,5-bis(4-aminophenoxy) phenyl] diphenylphosphine oxide (DATPPO)

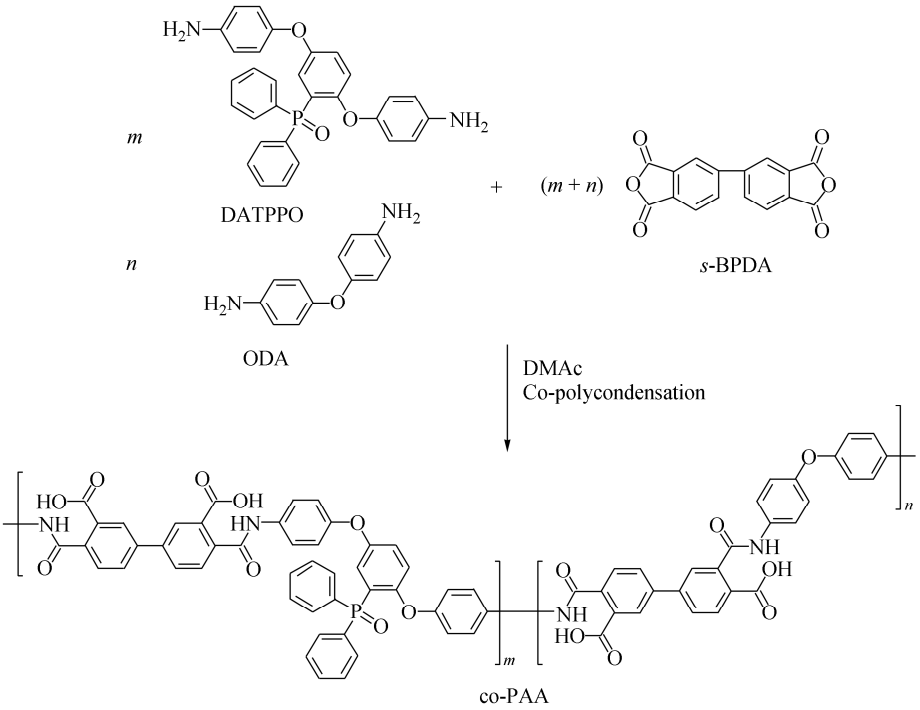


**Scheme 2** The reaction scheme of PAA solutions (*m*:*n* = 0:10 to 6:4)

### *Preparation of PI Fibers*

The PAA solution was filtrated and degassed prior to use. Dry-jet wet spinning process was adopted to prepare PAA fibers. The procedure is illustrated in Scheme 3. Typically, the PAA solutions were extruded with a spinneret with 50 holes and a 0.12 mm diameter into a coagulation bath (mixture of water and DMAc with a volume ratio of 42:58). The solidifying filament entered the washing bath, passed into the heating oven, and was

finally collected on the winders. The as-prepared PI fibers were synthesized by the PAA fibers heating to 300 °C and then drawn at different ratios to obtain the resulting PI fibers. The chemical reaction procedure is shown in Scheme 4.

**Table 1** Inherent viscosities of PAA solutions and mechanical properties of the PI fibers

| Polymer No. | DATPPO:ODA (molar ratio) | Draft/draw ratio | $\eta_{inh}$ (dL/g) | Mechanical properties | | |
|---|---|---|---|---|---|---|
| | | | | Strength (GPa) | Modulus (GPa) | Elongation at break (%) |
| PI-0 | 0:10 | 3.0/1.6 | 2.18 | 0.86 ± 0.05 | 14.01 ± 0.94 | 15.37 ± 0.49 |
| PI-1 | 1:9 | 3.0/1.6 | 2.04 | 0.83 ± 0.04 | 12.44 ± 0.90 | 21.72 ± 1.52 |
| PI-2 | 2:8 | 3.0/1.6 | 1.90 | 0.75 ± 0.03 | 11.21 ± 1.10 | 25.15 ± 2.27 |
| PI-3 | 3:7 | 3.0/1.6 | 1.80 | 0.69 ± 0.02 | 10.74 ± 0.76 | 28.09 ± 2.08 |
| PI-4 | 4:6 | 3.0/1.6 | 1.78 | 0.62 ± 0.04 | 9.85 ± 0.86 | 33.38 ± 2.36 |
| PI-5 | 5:5 | 3.0/1.6 | 1.65 | 0.48 ± 0.03 | 7.09 ± 0.61 | 35.91 ± 2.66 |
| PI-6 | 6:4 | 3.0/1.6 | 1.51 | 0.39 ± 0.04 | 6.66 ± 0.66 | 36.93 ± 2.24 |
| PI-6′ | 6:4 | 3.0/2.0 | 1.51 | 0.56 ± 0.35 | 4.27 ± 0.72 | 33.10 ± 5.37 |
| PI-6″ | 6:4 | 3.0/2.5 | 1.51 | 0.64 ± 0.04 | 10.02 ± 0.68 | 30.08 ± 7.45 |

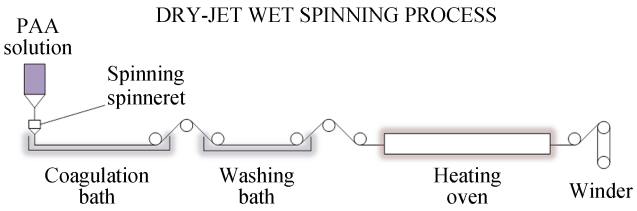


**Scheme 3** The dry-jet wet spinning process of PAA fibers

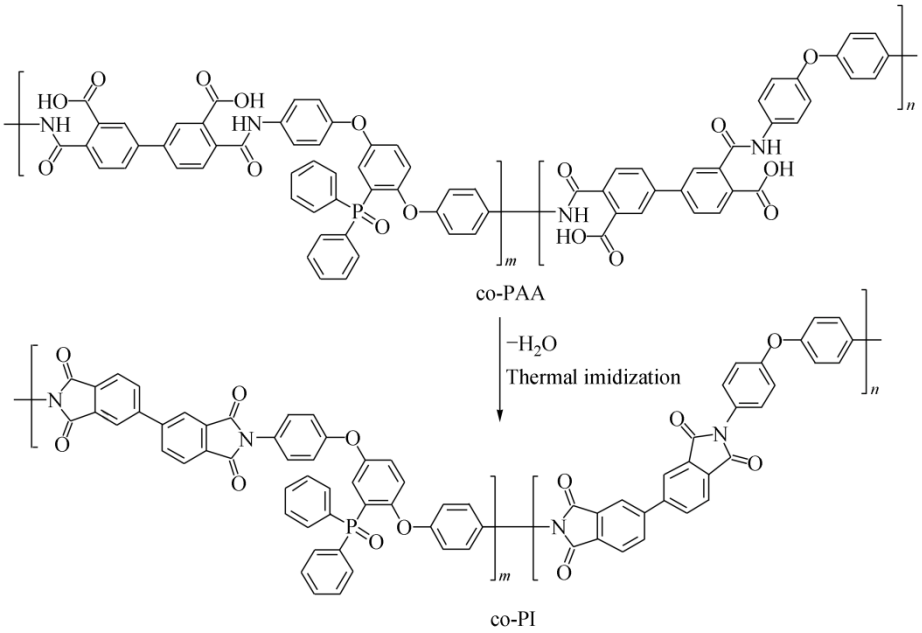


**Scheme 4** The thermal imidization procedure of PAA fibers

***Characterization***

FTIR measurement was performed with a VERTEX 70 spectrometer; the scanning wavenumber was in the range of 400–4000 $cm^{-1}$ for 32 scans. Nuclear magnetic resonance (NMR) spectra were recorded on a Bruker 400 spectrometer at 400 MHz for $^{1}$H-NMR, 162 MHz for $^{31}$P-NMR, and 101 MHz for $^{13}$C-NMR with tetramethylsilane as an internal standard. Melting points were determined with an XT-4 melting point apparatus.

Elemental analyses were conducted with an Elementar Vario EL cube (Elementar Corporation, Germany). The inherent viscosity ($\eta_{inh}$) of PAA was measured with an Ubbelohde viscometer with a capillary inner diameter of 0.5 mm at a concentration of 0.5 dL/g (dissolved in DMAc) at 30 °C. The mechanical properties of PI fibers were examined by a XQ-1 instrument with a gauge length and extension speed of 20 mm and 20 mm/min, respectively. For each group of fibers, at least 10 filaments were tested, and the average value was used as the final representative in accordance with GB/T 14337. The surface morphologies of the PI fibers were examined with an XL-30 environmental scanning electron microscope (ESEM) FEG (FEI Company). The samples were sprayed with Pt before observation. With the samples sealed in an aluminum pan, differential scanning calorimetry (DSC) was performed with a TA Q100 thermal analyzer. Glass transition temperatures ($T_g$s) were determined through DSC at a heating rate of 5 K/min and the temperature range of 50 °C to 350 °C. Dynamic mechanical analysis (DMA) was conducted with a Rheometric Scientific DMTA-V at 1 Hz and heating rate of 10 K/min at the temperatures ranging from 50 °C to 400 °C. Thermogravimetric analysis (TGA) was performed with a TA Q50 instrument at a heating rate of 10 K/min from 30 °C to 850 °C under nitrogen atmosphere. The limiting oxygen index (LOI) values were measured on an HC-2C oxygen index meter (Jingning Analysis Instrument Company, China). Wide-angle X-ray diffraction (WAXD) measurement was performed with a Bruker Advance AXS D8 using Cu K$\alpha$ radiation of $\lambda = 0.154$ nm. Small-angle X-ray scattering (SAXS) profiles were determined with Nanostar-u (Bruker AXS INC.) at a wavelength of 0.154 nm. A CCD X-ray detector (HI-STAR) was used at a distance of 1062 nm from the sample. The SAXS 2D images were processed with the FIT2D software package.

## RESULTS AND DISCUSSION

### *Synthesis of PAA Solutions*

A series of PAA solutions containing phenyl phosphorous oxide (PPO) groups were obtained after the reaction of *s*-BPDA with different molar ratios of DATPPO/ODA, which showed different viscosities. As shown in Table 1, the inherent viscosity declined from 2.18 dL/g to 1.51 dL/g with the increase of DATPPO content because the bulky side groups in the DATPPO monomer restricted the growth of molecular weight. During the experiment, it was found that when the molar ratio of mixed diamine (DATPPO/ODA) was higher than 6/4, the viscosity of the spinning solution was too low to spin the fibers.

### *Structure Characterization of PI Fibers Containing Phosphorous Groups*

The chemical structures of the PI fibers with different molar ratios of DATPPO/ODA were confirmed by FTIR, as shown in Fig. 1. All the PI fibers have four characteristic absorption peaks at 1771, 1712, 1368 and 736 $cm^{-1}$, attributed to the C=O asymmetrical stretching of imide groups, C=O symmetrical stretching of imide groups, C−N stretching, and C=O bending of the imide ring, respectively. Moreover, the characteristic absorption peaks of PAA fibers at 1660 and 1550 $cm^{-1}$ for the amide-I and the amide-II bands disappeared after thermal imidization, indicating the high imidization degree of the resulting PI fibers. Furthermore, the co-PI fibers exhibited absorption peaks at 1465 and 1191 $cm^{-1}$ for P=O groups, suggesting that the diamine DATPPO was successfully incorporated into the copolymer. The intensity of the P=O groups increased with increasing the DATPPO content.

### *Morphology of PI Fibers*

The surface and cross-sectional morphologies of the fibers were studied by SEM, as shown in Fig. 2. All the fibers showed homogenous and smooth surfaces with an average diameter of 18 μm and the circle-shape cross section without defects. These results were due to the balanced dual diffusion between the solvent and coagulant, and the appropriate concentration of the coagulation bath for the DATPPO/ODA/*s*-BPDA system. Overall, the spinning solutions of the DATPPO/ODA/*s*-BPDA system showed a good spinning performance through the dry-jet wet spinning process.

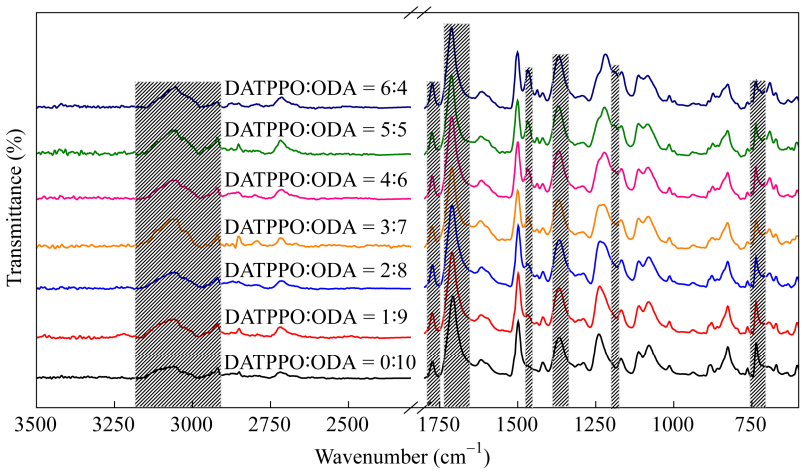


**Fig. 1** FTIR spectra of PI fibers with different molar ratios of diamine

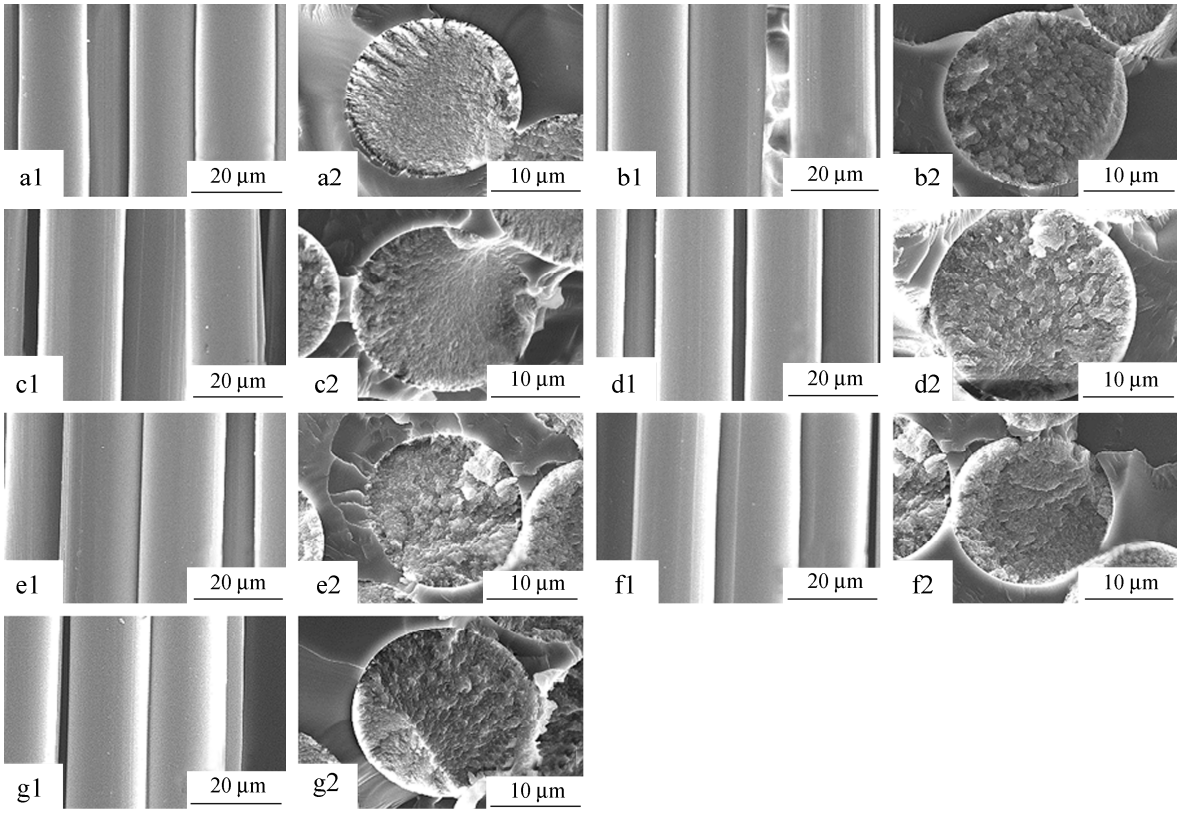


**Fig. 2** The surface and the cross-section morphologies of PI fibers: (a1, a2) PI-0, (b1, b2) PI-1, (c1, c2) PI-2, (d1, d2) PI-3, (e1, e2) PI-4, (f1, f2) PI-5 and (g1, g2) PI-6

### *Thermal Properties of the PI Fibers*

Figure 3 shows the thermal stabilities of the PI fibers heating from 400 °C to 850 °C at a rate of 10 K/min in the nitrogen atmosphere. The pure PI fiber (PI-0) exhibited only one decomposition region, and the other two were observed from the derived TGA curves of the co-PI fibers (Fig. 3b). Comparing the curves of derived TGA, the region at 600 °C belonged to the decomposition of imide chains, and the other one at 550 °C corresponded to the decomposition of P—C band in the co-PI fibers. All the fibers exhibited a similar decomposition behavior. The temperature of 5% and 10% weight loss ($T_{5\%}$ and $T_{10\%}$) and char yields at 850 °C are summarized in Table 2. The

temperatures of 5% and 10% weight loss ranged from 531 °C to 559 °C and from 551 °C to 583 °C, respectively. The residual weights at 850 °C ranged from 58% to 62% under the nitrogen atmosphere. The high char yields indicate that these fibers have good thermal stability. Furthermore, with the increase of DATPPO content, the intensity of the decomposition region at 550 °C increased, whereas the intensity of the decomposition region at 600 °C decreased. We also found that these two decomposition regions showed a simultaneous shift to the higher temperature (Fig. 3b).

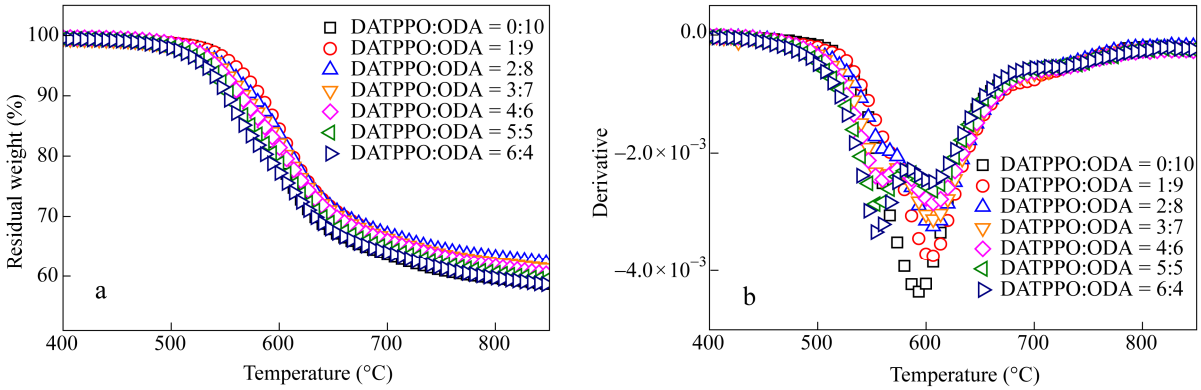


**Fig. 3** TGA curves of PI fibers with different diamine ratios

As well known, LOI is an important parameter to evaluate the flame retardancy of the materials. In the present work, the LOI of as-prepared PI fibers was calculated according to the Eq. (1) reported by van Krevelen in 1974[19].

$$\mathrm{LOI} = 17.5 + 0.4\mathrm{CR} \tag{1}$$

In the Eq. (1), CR is the char residue in wt% at 850 °C. As shown in Table 2, with the DATPPO content increased from 0% to 20%, the LOI values of PI fibers revealed an increase from 40.7% to 42.3%. However, when the DATPPO content increased continuously from 30% to 60%, the LOI values of PI fibers decreased from 41.9% to 40.7%. The results indicated the flame-retardant properties of the fibers dependent on the DATPPO content; especially, the negative effect was shown with increasing the DATPPO content over 30%. The reason was that at low content of DATPPO, the CR of PI fibers at 850 °C was increased. While at higher DATPPO content, the CR at 850 °C decreased because of the degradation of P—C bond. Additionally, the LOI values of the fibers were measured by oxygen index meter. According to Table 2, with the DATPPO content increasing from 0% to 20%, the LOI of the fibers showed a significant growth from 34.9% to 44.6%. However, when the DATPPO content was increased continuously to 60%, the LOI of fibers kept constant at an average value of 44.7%. Both the calculated and experimental results indicated that the as-prepared fiber exhibited an excellent flame retardancy.

**Table 2** Thermal behaviors of the PI fibers

| Polymer No. | DATPPO:ODA (molar ratio) | $T_{5\%}$ [a] (°C) | $T_{10\%}$ [a] (°C) | CR [b] (%) | LOI [c] (%) | LOI [d] (%) |
|---|---|---|---|---|---|---|
| PI-0 | 0:10 | 555 | 573 | 58 | 40.7 | 34.9 |
| PI-1 | 1:9 | 559 | 583 | 61 | 41.9 | 42.5 |
| PI-2 | 2:8 | 548 | 575 | 62 | 42.3 | 44.6 |
| PI-3 | 3:7 | 544 | 567 | 61 | 41.9 | 44.6 |
| PI-4 | 4:6 | 542 | 564 | 60 | 41.5 | 44.6 |
| PI-5 | 5:5 | 533 | 555 | 59 | 41.1 | 44.7 |
| PI-6 | 6:4 | 531 | 551 | 58 | 40.7 | 44.8 |

[a] Temperature of 5% or 10% weight loss under $N_2$; [b] Weight retention of the fibers at 850 °C under $N_2$; [c] Values obtained by theoretical calculation; [d] Values measured by oxygen index meter

The $T_g$s of the PI fibers were investigated through DSC and DMA, as shown in Fig. 4. The values of $T_g$ are 263, 264, 269, 278, 279, 276, and 274 °C, which correspond to the DATPPO/ODA molar ratios of 0/10, 1/9, 2/8, 3/7, 4/6, 5/5, and 6/4, respectively (Fig. 4a). In Fig. 4(b), the $\alpha$ relaxation of the polymer chains corresponds to the glass transition temperatures, and all the $T_g$s of the co-PI fibers are higher than that of the blank one (PI-0). With the increase of DATPPO content from 0% to 40%, the values of $T_g$ increased from 263 °C to 279 °C. When the DATPPO content increased to 60% continuously, the $T_g$ value decreased to 274 °C. Increase of DATPPO content resulted in the growth of the branched degree of the polymer chains. Consequently, the movement of the molecular chains was confined. However, with the increase of branched chains, the regularity of the molecular segments decreased, and the interactions among molecules weakened. The results of DMA (shown in Fig. 4b) are consistent with those of DSC. The $T_g$ values from DMA were 258, 265, 265, 266, 269, 269, and 265 °C, which correspond to the DATPPO/ODA molar ratios of 0/10, 1/9, 2/8, 3/7, 4/6, 5/5 and 6/4, respectively.

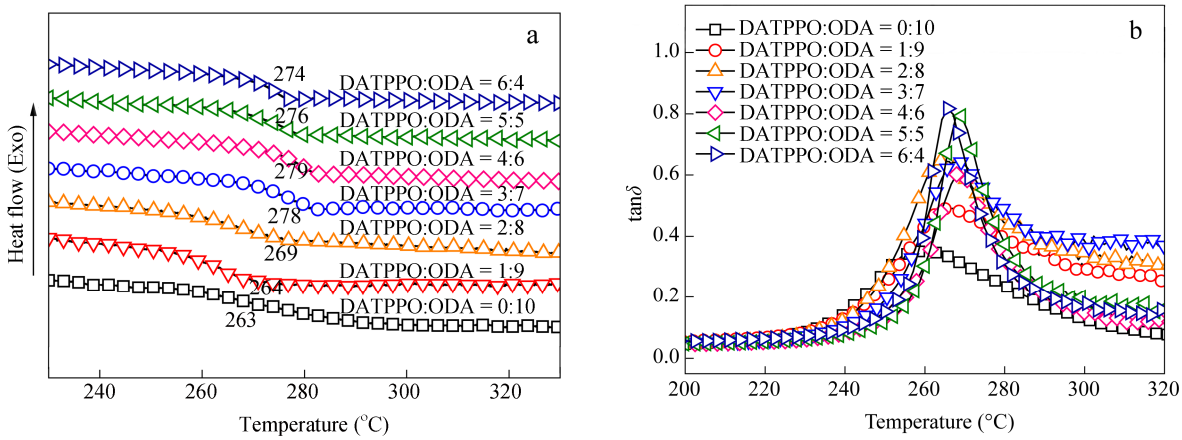


**Fig. 4** Glass transition temperatures of PI fibers from (a) DSC and (b) DMA

***Mechanical Properties of the PI Fibers***

Mechanical property is a crucial parameter for the polymeric fibers in the engineering applications. As shown in Figs. 5 and 6, the mechanical properties of the PI fibers varied with DATPPO contents and draw ratios. The details are provided in Table 1. It revealed that the homo-PI fibers (PI-0) possessed a higher tensile strength and the initial modulus of 0.86 and 14.01 GPa compared with co-PI. However, with the incorporation of DATPPO into the structural backbones, both tensile strength and initial modulus decreased dramatically, whereas elongation at break increased greatly. Actually, the original order degree of ODA/BPDA system was disturbed by the introduction of DATPPO into the molecular structure, which impaired the intermolecular interactions. As a result, the strength and modulus of the fibers were reduced with the increase of the monomer DATPPO content. In Table 1, the values of tensile strength and initial modulus of the PI fibers ranged from 0.86 GPa to 0.39 GPa, and from 14.01 GPa to 6.66 GPa, respectively, under the same processing conditions. The elongations ranged from 15.37% to 36.93%. Figure 6 shows the effect of draw ratio on the tensile strength, initial modulus and elongation at break of PI-6 fibers. The tensile strength ranged from 0.39 GPa to 0.64 GPa, the initial modulus ranged from 6.66 GPa to 10.02 GPa, and elongation ranged from 36.93% to 30.08%. The results above mentioned indicated that the increase of the draw ratio could improve the mechanical properties.

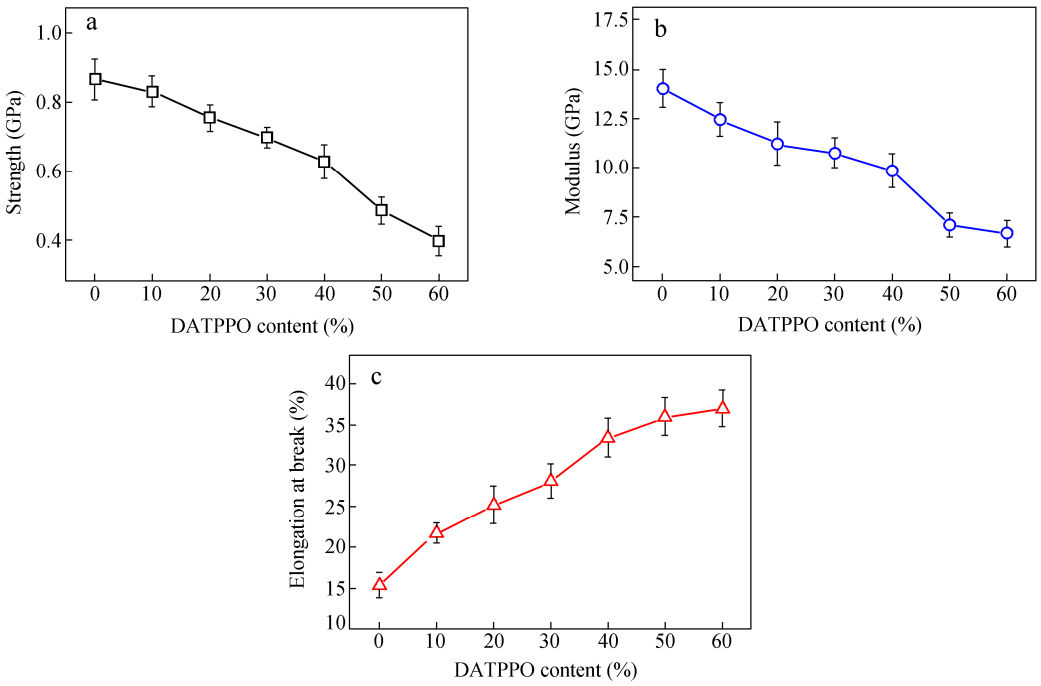


**Fig. 5** The mechanical properties of PI fibers with different DATPPO contents

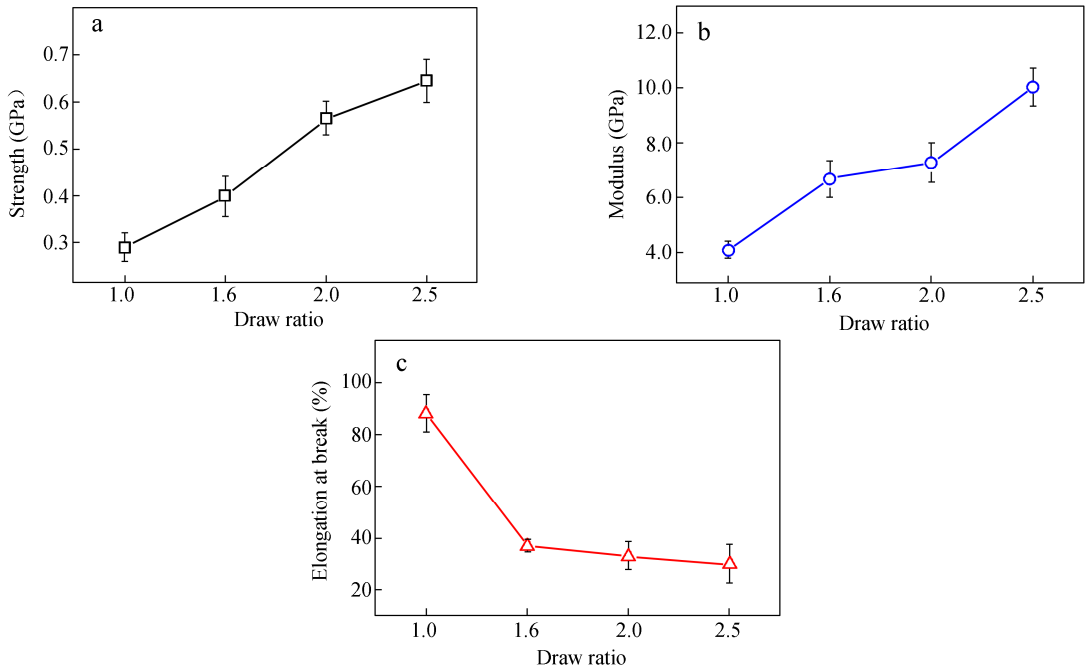


**Fig. 6** Effect of draw ratio on the (a) tensile strength, (b) initial modulus and (c) elongation at break of PI-6 fibers

### *Molecular Packing of PI Fibers*

WAXD measurement was performed to investigate the molecular packing of the PI fibers. Two of the structure parameters, orientation and crystallinity in the fibers, played important roles in the polymeric fibers. 1D WAXD intensity profiles along the parallel and perpendicular to the fiber axis are shown in Fig. 7. A group of broad peaks in the range of 12°–15° were observed for the pure PI and co-PI fibers before and after drawing, which indicated that all the PI fibers were amorphous. In order to understand the structural evolution of the fibers

during the drawing process, the order degrees of macromolecules in the PI fibers with the amorphous structure were evaluated by the following Eq. (2) according to Wu's report[20]

$$X = \frac{U_0}{I_0} \times \frac{U_x}{I_x} \times 100\% \tag{2}$$

where $X$ is defined as the order degree, and $U_0$ and $U_x$ denote the backgrounds of the reference and experimental samples, whereas $I_0$ and $I_x$ are integral intensities of diffraction lines of the reference and experimental samples, respectively. The corresponding order degree values of PI fibers with various draw ratios (*i.e.* 1.0, 1.6, 2.0 and 2.5) are calculated as 1.92 $U_0/I_0$, 2.06 $U_0/I_0$, 2.13 $U_0/I_0$, 2.29 $U_0/I_0$, respectively, which gives an evidence of higher order degree of lateral packing with increasing draw ratio. Actually, the results indicate that the high orientation of the amorphous matter makes a main contribution to improving the mechanical properties of the PI fibers.

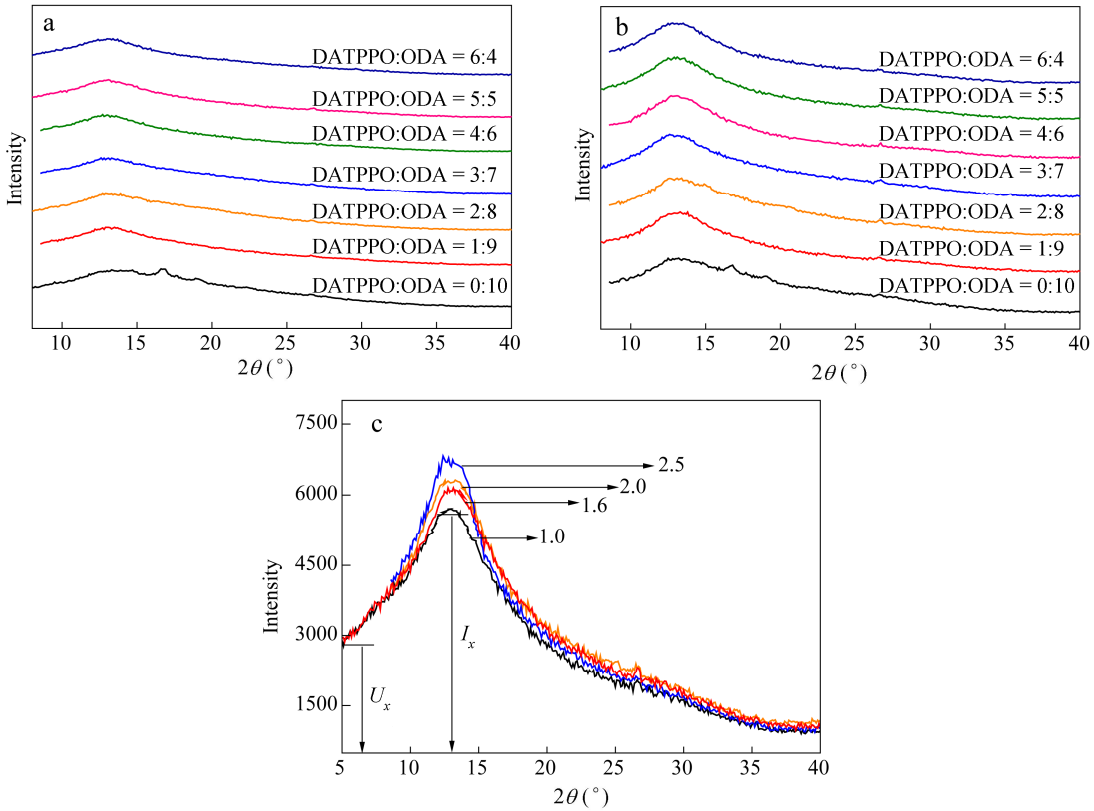


**Fig. 7** 1D WAXD profiles of the fibers (a) along the parallel, (b) perpendicular to fiber axis and (c) fibers of PI-6 with drawing perpendicular to fiber axis

### *Micro-morphological Changes in Fibers*

The corresponding morphological changes extracted with the SAXS technique were also examined. Figure 8 shows 2D SAXS patterns of PI-6 with different draw ratios. SAXS scattering is mainly due to the existence of microvoids in the PI fibers[21]. Microvoids were generated during the non-equilibrium dual diffusion and the thermal imidization process for releasing small molecules, which affect the mechanical properties of the PI fibers. The common feature was that SAXS intensity had a streak shape along the meridian, and no detectable scattering was observed along the equator direction. The streak showed that the superstructure (crystalline fibrils or voids as reported by Vickers[22]) of PI fibers mainly consisted of microvoids. The result is somewhat different from those of studies on crystalline PI fibers[23–25]. In our case, the samples were completely amorphous, so streak scattering was related to the microvoids. To obtain information on the average length of microvoids and

misorientation of the fiber axis, the following Eq. (3) proposed by Ruland was used.

$$B_{\text{obs}} = \frac{2\pi}{Lq} + B_{\Phi} \text{.....(Cauchy-Cauchy)} \quad (3)$$

where $B_{\text{obs}}$ is actually the full width at half maximum of the azimuthal profile from the streak fitted with a Lorentzian function, $q = 4\pi\sin\theta/\lambda$ is the scattering vector, $2\theta$ is the scattering angle, and $\lambda$ is the X-ray wavelength.

Streak length increased with the evolution of draw ratio, as shown in Fig. 8, which indicated that the size of the microvoids gradually decreased. The Ruland plots of PI-6 with different draw ratios were adopted to quantify the changes (Fig. 9). The corresponding results are presented in Table 3. The streak on the equator was produced by the scattering objects extended along the fiber direction. The microvoids size distribution and the misorientation of the scattering objects contributed to streak scattering. As shown in Table 3, the length of microvoids decreased with the increase in draw ratios (varying from 538 nm to 428 nm). Meanwhile, the misorientation ($B_{\Phi}$) degree also decreased from 14.3° to 3.5° with the increase of draw ratios. These results show that increasing the draw ratio is beneficial to the elimination of defects and molecular orientation, which give rise to increased tensile strength and modulus.

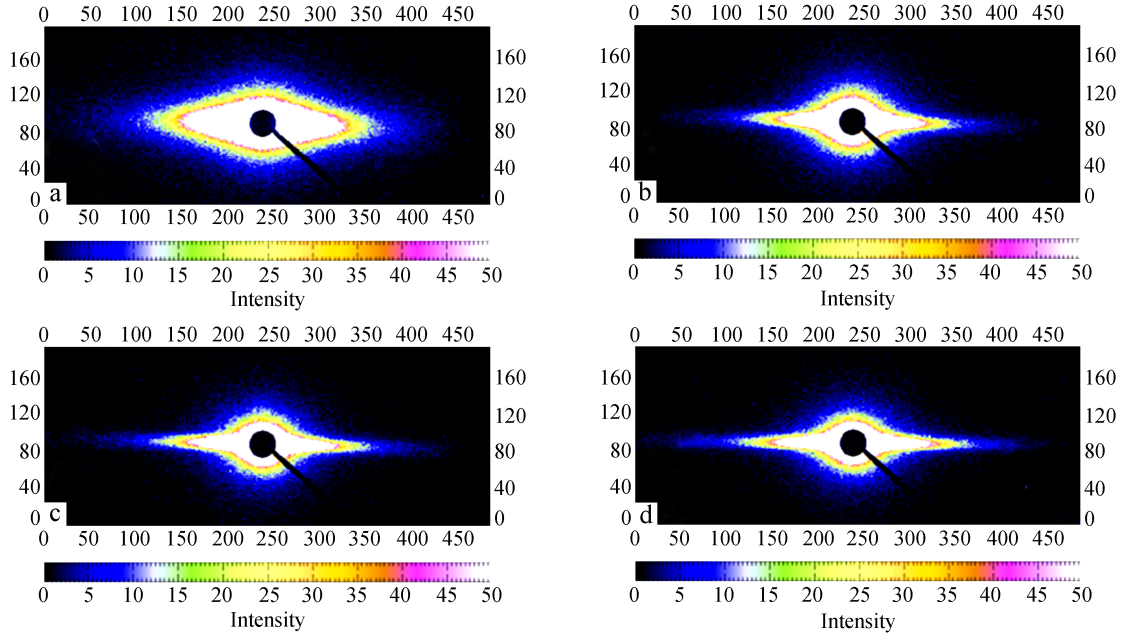


**Fig. 8** 2D SAXS patterns of PI fibers at draw ratios of (a) 1.0, (b) 1.6, (c) 2.0 and (d) 2.5

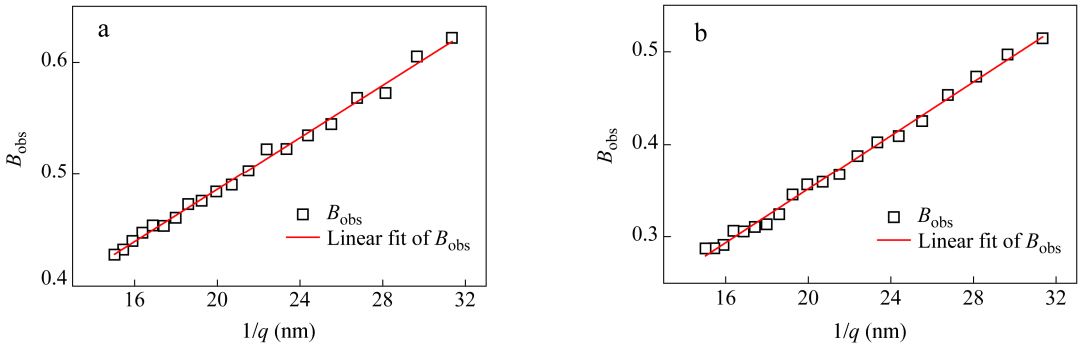


**Fig. 9** Ruland plots of PI-6 at draw ratios of (a) 1.0 and (b) 2.5

As reported by Zhang *et al.*[26], the radius of microvoids with cross-section could be described by Guinier functions, as following Eq. (4). The Guinier plots of the scattering intensities along the equatorial streak were obtained according to the streak of meridional direction. Then a new Guinier plot was determined by subtracting the tangent curve until the final plot becoming a straight line, as shown in Fig. 10. The radius of the microvoids can be calculated by the tangent value according to the Eq. (4) and the results are listed in Table 3. Obviously, the radius of the microvoids in the fibers showed multi-order cross-section characteristics, depending on the drawing ratios. For the results of Guinier plots, we found that the radius decreased with the increase of drawing ratios, which indicated that the higher draw ratio could make the voids being shorter length and smaller radius, namely a process to eliminating the defects.

$$I(q) = I(0)\exp\left(\frac{-q^2R^2}{5}\right) \tag{4}$$

where $R$ is the radius of microvoids with circular cross-section, $q$ ($q = 4\pi\sin\theta/\lambda$) is the scattering vector, $2\theta$ is the scattering angle and $\lambda$ is the wavelength.

**Table 3** Microvoid parameters of the PI-6 fibers with different draw ratios

| Draw ratio | $R1$ (nm) | $R2$ (nm) | $R3$ (nm) | $L$ (nm) | $B_\Phi$ (rad) | $B_\Phi$ (°) |
|---|---|---|---|---|---|---|
| 1.0 (As-spun) | 1.27 | 3.35 | 7.19 | 538 | 0.25 | 14.3 |
| 1.6 | 1.03 | 2.84 | 6.24 | 436 | 0.11 | 6.5 |
| 2.0 | 0.80 | 2.68 | 4.73 | 433 | 0.07 | 4.2 |
| 2.5 | 0.84 | 2.35 | 5.07 | 428 | 0.06 | 3.5 |

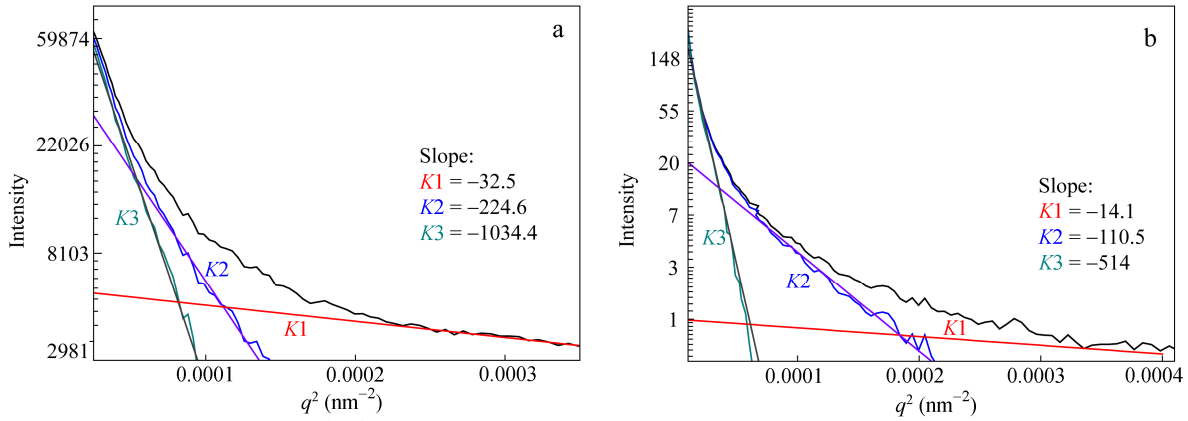


**Fig. 10** Guinier plots of the scattering intensities along the meridian direction with draw ratios equal to (a) 1.0, (b) 2.5 ($K1$: measured values; $K2$: values after subtracting the resolved curve $K1$; $K3$: values after subtracting the resolved curve $K1$ and $K2$)

**Table 4** Solubility of the PI fibers

| Polymer No. | DATPPO:ODA (molar ratio) | Solvents [a] | | | | | | | | |
|---|---|---|---|---|---|---|---|---|---|---|
| | | NMP | DMAc | DMF | THF | TFA | DMF/LiCl | $CCl_4$ | DMSO | EtOH |
| PI-0 | 0:10 | − | − | − | − | − | − | − | − | − |
| PI-1 | 1:9 | − | − | − | − | − | − | − | − | − |
| PI-2 | 2:8 | − | − | − | − | − | − | − | − | − |
| PI-3 | 3:7 | − | − | − | − | − | − | − | − | − |
| PI-4 | 4:6 | − | − | − | − | − | − | − | − | − |
| PI-5 | 5:5 | − | − | − | − | − | − | − | − | − |
| PI-6 | 6:4 | − | − | − | − | +− | − | − | − | − |

[a] ++, wholly soluble; +−, partially soluble; −, insoluble

***Solubility of PI Fibers***

The solubility of PI fibers in the solvents (NMP, DMAc, DMF, THF, TFA, DMF/LiCl, $CCl_4$, DMSO and EtOH) was investigated by dipping 0.001 g of PI fibers in 20 mL solvents. As shown in Table 4, all the fibers showed high resistance to these solvents except for the PI-6 fiber which was partially dissolved in TFA. These results indicated that the as-prepared polyimide fibers exhibited high resistance to the solvents.

## CONCLUSIONS

A series of PAA fibers containing PPO groups in the side chains were successfully fabricated with DATPPO monomer through the dry-jet wet spinning process. The corresponding PI fibers with smooth surfaces were obtained through thermal imidization of the PAA fibers. The following conclusions were obtained.

(1) With the increase of DATPPO content, the $T_g$s of the PI fibers increased from 263 °C to 279 °C and then decreased from 279 °C to 274 °C. The maximum value of $T_g$s was observed at DATPPO/ODA molar ratio equal to 4/6.

(2) The TGA results showed that the residual char yields of the PI fibers were in the range of 58% to 62%. This residual char yield range indicated good thermal stability of the fibers. The higher LOI values showed that the co-PI fibers possessed a better flame-retardant.

(3) Compared with those of the pure PI fiber, the mechanical properties of the co-PI fibers decreased with the increase of DATPPO contents. When the draw ratios were increased, the mechanical properties were improved.

(4) The WAXD and SAXS patterns indicated that heat drawing could eliminate defects and increase the orientation of the polymer chains but had no effect on the solid state. Consequently, the increase of mechanical properties was entirely attributed to the orientation of the amorphous matter.

(5) The solubility test showed that all the fibers possessed high resistance to the solvents.

## REFERENCES

1 Samuel, I.R. and Edgar, S.C., 1968, U.S. Pat., 3,415,782
2 Cheng, S.Z.D., Wu, Z., Eashoo, M., Hsu, S.L.C. and Harris, F.W., Polymer, 1991, 32(10): 1803
3 Eashoo, M., Shen, D., Wu, Z., Lee, C.J., Harris, F.W. and Cheng, S.Z.D., Polymer, 1993, 34(15): 3209
4 Koontz, S.L., Leger, L.J., Visentine, J.T., Hunton, D.E., Cross, J.B. and Hakes, C.L., J. Spacecraft Rockets, 1995, 32(3): 483
5 Grossman, E., Lifshitz, Y., Wolan, J.T., Mount, C.K. and Hoflund, G.B., J. Spacecraft Rockets, 1999, 36(1): 75
6 Dong, J., Yin, C., Luo, W. and Zhang, Q., J. Mater. Sci., 2013, 48(21): 7594
7 Fang, G., Li, H., Liu, J., Ni, H., Yang, H. and Yang, S., Chem. Lett., 2015, 44(8): 1083
8 Eashoo, M., Wu, Z., Zhang, A., Shen, D., Tse, C., Harris, F.W., Cheng, S.Z.D., Gardner, K.H. and Hsiao, B.S., Macromol. Chem. Phys., 1994, 195(6): 2207
9 Yin, C., Dong, J., Li, Z., Zhang, Z. and Zhang, Q., Compos. Part B-Eng., 2014, 58: 430
10 Shen, Z., Mu, Y., Ding, Y., Liu, Y. and Zhao, C., Study on the mechanical property of polyimide film in space radiation environments; proceedings of the Selected Proceedings of the Chinese Society for Optical Engineering Conferences held November 2015, International Society for Optics and Photonics, 2016.
11 Yokota, K., Abe, S., Tagawa, M., Iwata, M., Miyazaki, E., Ishizawa, J.I., Kimoto, Y. and Yokota, R., High. Perform. Polym., 2010, 22: 237
12 Duo, S.W., Song, M.M., Liu, T.Z., Hu, C.Y. and Li, M.S., Key Eng. Mater., 2012, 492: 521
13 Liu, R. and Ma, J.D., Sichuan Text Technology (in Chinese), 2004, 4: 47
14 Ding, X., Qiu, X., Ma, X., Li, G. and Gao, L., Chemistry Journal of Chinese Universities (in Chinese), 2013, 34: 2650
15 Zhao, Y., Feng, T., Li, G., Liu, F., Dai, X., Dong, Z. and Qiu, X., RSC Adv., 2016, 6(48): 42482

16 Hergenrother, P.M., Watson, K.A., Smith, J.G., Connell, J.W. and Yokota, R., Polymer, 2002, 43(19): 5077
17 Connell, J.W., Smith, J.G., Hergenrother, P.M., Watson, K.A. and Thompson, C.M., 2003, U.S. Pat., 7,109,287
18 Hergenrother, P.M., Smith, J.G., Connell, J.W. and Watson, K.A., 2005, U.S. Pat., 6,958,192
19 van Krevelen, D.W., Polymer, 1975, 16(8): 615
20 Zhang, M., Niu, H., Lin, Z., Qi, S., Chang, J., Ge, Q. and Wu, D., Macromol. Mater. Eng., 2015, 300(11): 1096
21 Chang, J., Niu, H., He, M., Sun, M. and Wu, D., J. Appl. Polym. Sci., 2015, 132(34): 42474
22 Vickers, M.E., Briggs, N.P., Ibbett, R.N., Payne, J.J. and Smith, S.B., Polymer, 2001, 42(19): 8241
23 Dong, J., Yin, C., Zhang, Z., Wang, X., Li, H. and Zhang, Q., Macromol. Mater. Eng., 2014, 299(10): 1170
24 Yin, C., Dong, J., Zhang, D., Lin, J. and Zhang, Q., Eur. Polym. J., 2015, 67: 88
25 Yin, C., Dong, J., Zhang, Z., Zhang, Q. and Lin, J., J. Polym. Sci., Part B: Polym. Phys., 2015, 53(3): 183
26 Dong, J., Yin, C., Lin, J., Zhang, D. and Zhang, Q., RSC Adv., 2014, 4(84): 44666